Slow Decay of Correlations in Non-hyperbolic Dynamical Systems

Department of Applied Physics, Osaka City University
Tomoshige MIYAGUCHI [1]

1 Introduction

In the past decades, a lot of studies have been devoted to investigations of the relations between microscopic chaos and non-equilibrium behavior such as relaxation and transport, and it has been found that microscopic chaos plays essential roles in non-equilibrium processes [12, 13]. For example, it is well known that, for fully chaotic (hyperbolic) systems, correlation functions decay exponentially and their decay rates are characterized by the discrete eigenvalues of its Frobenius–Perron (FP) operator [27, 28, 31, 30, 32]. As one of the examples of the hyperbolic systems that permits detailed calculations, the baker transformation has been studied extensively and its spectral properties of FP operator are fully understood [19]. In addition, the baker map is considered as an abstract model of chaotic Hamiltonian systems, because it has the area-preserving property, which is a universal feature of the Poincaré map of the Hamiltonian systems of two degrees of freedom [5]. In fact, similarities of the baker map to the Lorentz gas with finite horizon have been pointed out [37].

In contrast to the hyperbolic systems, dynamics in generic Hamiltonian systems is more complicated and diverse. In fact, when a phase space of a Hamiltonian system consists of integrable (torus) and non-integrable components (chaos), power law decays of correlations are frequently observed [11, 15, 20, 22, 23, 26, 38]. Although such kind of systems, i.e., systems with mixed type phase spaces, are more generic than the integrable or the fully chaotic systems, the theoretical understanding of their statistical properties is not enough; for example the ergodic and mixing properties of chaotic components of generic systems are still unclear from the theoretical point of view.

In order to understand the mechanism of the sub-exponential decay of correlation functions in dynamical systems, non-hyperbolic one-dimensional maps have been studied by several authors [1, 2, 6, 7, 14, 15, 18, 8, 34, 35, 36]. In particular, Tasaki and Gaspard introduced piecewise linear versions of non-hyperbolic one-dimensional maps in [34, 35, 36], and showed that the correlation

[1]E-mail: t.mygch@gmail.com

functions for a class of smooth observables exhibit a sub-exponential decay. Thus, it is natural to imagine a close connection of these non-hyperbolic maps and mixed type Hamiltonian systems. Here, we review our work [24] in which we proposed a modified version of the above-mentioned Tasaki-Gaspard piecewise linear map [34, 35] and extend it to an area-preserving system. We also point out a connection with a billiard system called the mushroom billiard [9, 10], which also shows sub-exponential decay of correlations [25].

Our theoretical treatment is mainly based on Refs. [34, 35], where a piecewise linear version of the Pomeau-Manneville map [21, 29] is proposed and its generalized spectral properties of the FP operator in a sense of Refs. [16, 17] have been elucidated. In particular, they have analytically derived a generalized spectral decomposition (the spectral decomposition in terms of generalized functions) of the FP operator. Their model has a marginally unstable fixed point (MUFP) and exhibits power law decays of correlations which they have found to be an outcome of a continuous spectrum of the FP operator. In addition to the MUFP, the piecewise linear map studied in the present paper has a singular structure, which suppresses injections of the orbits into neighborhoods of the MUFP. Due to this property, the uniform density is invariant under time evolution and the map can be extended to an area-preserving map on the unit square.

2 A Piecewise Linear Intermittent Map

2.1 Definition

The dynamical system we study in this paper is the piecewise linear map shown in Fig. 1. This map $\phi(x) : [0,1) \to [0,1)$ consists of the left $0 < x < b$ and the right $b < x < 1$ parts. Each part is formed by the infinite number of line segments; the circles plotted in Fig. 1 indicate endpoints of these line segments. The map $\phi(x)$ is defined by

$$\phi(x) = \begin{cases} \eta_k^-(x - \xi_k^-) + \xi_{k-1}^- & \text{for } x \in [\xi_k^-, \xi_{k-1}^-) \quad (k = 1, 2, \cdots), \\ \eta_k^+(x - \xi_k^+) + \xi_{k-1}^- & \text{for } x \in [\xi_k^+, \xi_{k-1}^+) \quad (k = 1, 2, \cdots). \end{cases} \tag{1}$$

In this definition, ξ_k^- $(k = 0, 1, \cdots)$ represent the horizontal coordinates of the endpoints of the line segments for the left part $(x < b)$. And they are defined by

$$\begin{aligned} &\xi_0^- = b, \\ &\xi_{k-1}^- - \xi_k^- = \frac{b}{\zeta(\beta)} \left(\frac{1}{k}\right)^\beta \quad (k = 1, 2, \cdots), \end{aligned} \tag{2}$$

where $\beta > 1$ is a parameter. Furthermore, η_k^- is the slope of the k-th line segment and defined as

$$\eta_k^- = \frac{\xi_{k-2}^- - \xi_{k-1}^-}{\xi_{k-1}^- - \xi_k^-} = \begin{cases} \frac{1-b}{b}\zeta(\beta) & (k = 1), \\ \left(\frac{k}{k-1}\right)^\beta & (k = 2, 3, \cdots), \end{cases} \tag{3}$$

where we set $\xi_{-1}^{-}=1$ for convenience. This definition of the left part $(0<x<b)$ is the same as that of the piecewise linear Pomeau-Manneville map proposed by Tasaki and Gaspard [34, 35]. The map can be approximated as $\phi(x)\sim x+Cx^{\frac{\beta}{\beta-1}}$ when $x\to 0+$, where C is a constant. Thus the origin $x=0$ is a MUFP and chaotic orbits stay near this MUFP for long times (sticking motions).

In the same way, ξ_k^+ $(k=0,1,\cdots)$ are the horizontal coordinates of the endpoints on the right part $(x>b)$ and defined as

$$\begin{aligned}&\xi_1^+=b\left(1+\tfrac{1}{\zeta(\beta)}\right),\quad \xi_0^+=1,\\ &\xi_{k-1}^+-\xi_k^+=\tfrac{b}{\zeta(\beta)}\left\{\tfrac{1}{(k-1)^\beta}-\tfrac{1}{k^\beta}\right\}\qquad \text{for}\quad k=2,3\cdots,\end{aligned}\tag{4}$$

and η_k^+ is the slope of the k-th line segment and defined as

$$\eta_k^+=\tfrac{\xi_{k-2}^--\xi_{k-1}^-}{\xi_{k-1}^+-\xi_k^+}=\begin{cases}\frac{1-b}{1-b(1+1/\zeta(\beta))} & (k=1),\\ \frac{k^\beta}{k^\beta-(k-1)^\beta} & (k=2,3,\cdots).\end{cases}\tag{5}$$

This is the definition of the right part of the map $\phi(x)$, $b<x<1$. This part is different from the Pomeau-Manneville type maps, but similar to a map proposed by Artuso and Cristadoro [7]. $\phi(x)$ behaves as $\phi(x)\sim(x-b)^{\frac{\beta-1}{\beta}}$ when $x\to b+$. Therefore the derivative $\phi'(x)$ of the map is divergent at $x=b$. We also assume that $\eta_1^+>0$, i.e. $b<\zeta(\beta)/(1+\zeta(\beta))$ holds.

Note that the uniform density on the interval $[0,1]$ is invariant under the time evolution of this map and thus the relations $1/\eta_k^+ + 1/\eta_k^- = 1$ are satisfied for $k=1,2,\cdots$. Figure 1 shows the shape of the map $\phi(x)$ for $\beta=1.3$ and $b=0.5$. This system can be easily extended to an two-dimensional area-preserving map, whose dynamics of the expanding direction is given by the map $\phi(x)$ (see below).

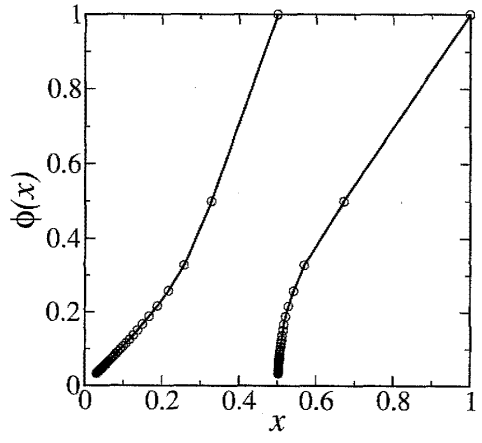

Figure 1: The piecewise linear map $\phi(x)$ for $b=0.5$ and $\beta=1.3$. The circles indicate endpoints of the linear segments.

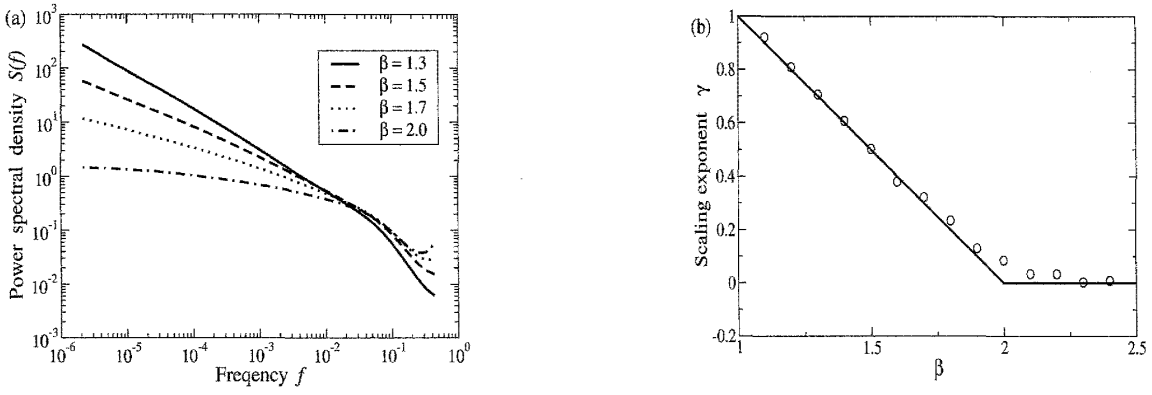

Figure 2: The power spectral densities (PSDs) of $x(t)$ (log-log plot) for four different values of the exponent $\beta : \beta = 1.3,\ 1.5,\ 1.7,\ 2.0$. These PSDs are obtained by 5000 realizations of the time series $x(t)$. (b) The scaling exponent γ of the PSD $S(f) \sim 1/f^{\gamma}$ as a function of the exponent β. The circles are the numerical results obtained by least square fittings in a low frequency region (below $f = 10^{-4}$) of the PSDs $S(f)$; and the solid line is the theoretical prediction.

2.2 Theoretical and Numerical Results

Figure 2(a) shows power spectral densities $S(f)$ of time series $x(t)$ produced by the map $\phi(x)$ as $x(t+1) = \phi(x(t))$. The power spectral densities in Fig. 2(a) exhibit clear $1/f^{\gamma}$ scalings in low frequency regions. In Fig. 2(b), the scaling exponent γ of the power spectrum $S(f) \sim 1/f^{\gamma}$ is plotted as a function of the exponent β. A theoretical prediction is shown by a dashed line in Fig. 2(b), which is obtained by the generalized spectral decomposition of the Frobenius-Perron operator of the map $\phi(x)$ (For a derivation, see [24].). Obviously, the numerical results are consistent with the theoretical prediction.

2.3 Area-Preserving Extension

The one-dimensional map $\phi(x)$ can be extended to an area-preserving two-dimensional transformation defined on the unit square $[0,1) \times [0,1)$ [24]. This extension $\psi(x,y) : [0,1) \times [0,1) \to [0,1) \times [0,1)$ is defined as

$$(x', y') = \psi(x,y) = \begin{cases} \left(\eta_k^-(x - \xi_k^-) + \xi_{k-1}^-,\ \dfrac{y}{\eta_k^-}\right) & \text{for } x \in [\xi_k^-, \xi_{k-1}^-), \\ \left(\eta_k^+(x - \xi_k^+) + \xi_{k-1}^-,\ \dfrac{y}{\eta_k^+} + \dfrac{1}{\eta_k^-}\right) & \text{for } x \in [\xi_k^+, \xi_{k-1}^+) \end{cases} \tag{6}$$

where $k = 1, 2, \cdots$. Obviously, the transformation for the horizontal coordinate x is the same as the map $\phi(x)$ defined by Eq. (1) and does not depend on the vertical coordinate y. This relation between one-dimensional map $\phi(x)$ and its area-preserving extension $\psi(x,y)$ is the same as that between the Bernoulli and the baker transformations. The phase space (i.e. the unit cell) of

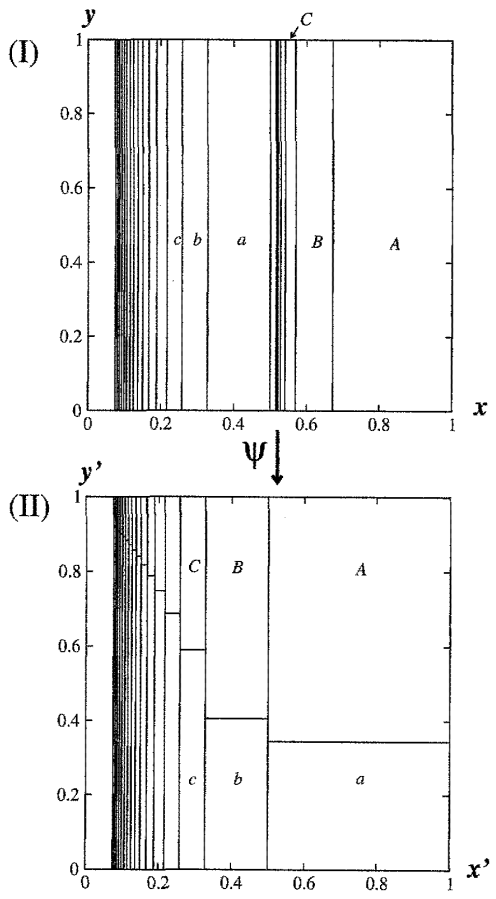

Figure 3: The area-preserving map $\psi(x,y)$ defined by Eq. (6) for $b = 0.5$ and $\beta = 1.3$. The domains with labels {A, B, C, a, b, c} in the upper cell (I) are mapped into the domains with the same labels in the lower cell (II), respectively. Each domain is uniformly stretched in the horizontal direction and uniformly squeezed in the vertical direction, but stretching and squeezing rates are different for different domains. There are infinite number of such domains, in other words, there exists an infinite partition. The domains are displayed only for the region $\{x \in [\xi_{15}^-, \xi_0^-]\}$ and $\{x \in [\xi_6^+, \xi_0^+]\}$ in the upper cell (I); only for $\{x \in [\xi_{15}^-, \xi_0^+]\}$ in the lower (II). The other regions are not displayed because the structures are too fine to see.

this area-preserving map can be partitioned into infinite pieces like

$$[0,1)^2 = \bigcup_{k=1}^{\infty} \{(x,y)|x \in [\xi_k^-, \xi_{k-1}^-), y \in [0,1)\} \cup \bigcup_{k=1}^{\infty} \{(x,y)|x \in [\xi_k^+, \xi_{k-1}^+), y \in [0,1)\}.$$

[See Fig. 3(I).] By the map $\psi(x,y)$, each domain of this partition $\{(x,y)|x \in [\xi_k^{\pm}, \xi_{k-1}^{\pm}), y \in [0,1)\}$ is uniformly stretched in the horizontal direction, and uniformly squeezed in the vertical direction, but stretching and squeezing rates are different for different domains . Then, domains $\{(x,y)|x \in [\xi_k^-, \xi_{k-1}^-), y \in [0,1)\}$ are mapped to the bottom part of the unit cell (domains $a, b, c, ...$) and the other domains $\{(x,y)|x \in [\xi_k^+, \xi_{k-1}^+), y \in [0,1)\}$ are mapped to the upper part (domains $A, B, C, ...$) as shown in Fig. 3(II). We call this upper part (domains $A, B, C, ...$) in Fig. 3(II) an *injection domain*. We also note that Fig. 3(I) can be viewed as an infinite partition of the phase space (the unit square) in terms of escape time, i.e., each rectangle region $(a, b, c, ...)$ has its own escape time. Here, we say that "a trajectory escapes" as it reaches the region $A, B, C, ...$ in Fig. 3(I).

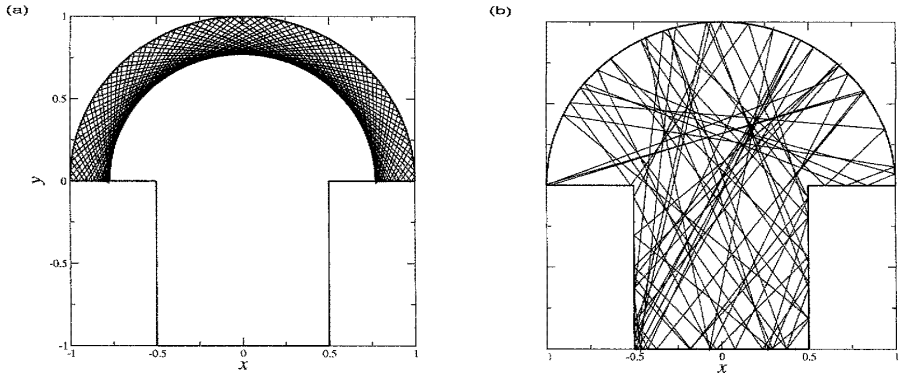

Figure 4: The shape of the table of the mushroom billiard, which consists of a half disk (the cap) and a rectangle (the stem). A point particle inside the table moves freely except for the elastic collisions with the walls. (a) A regular trajectory (torus) and (b) a chaotic trajectory are displayed.

3 Mushroom Billiard

In the previous sections, we introduced an abstract dynamical system which is area-preserving and shows a sub-exponential decay of correlations. But, is there a more realistic system with the similar structure? To answer this question, we further review our another paper [25], in which we studied a billiard system called the mushroom billiard.

The mushroom billiard is defined by the motion of a point particle on the billiard table depicted in Fig. 4. This table consists of a half disk of radius R (the *cap*) and a rectangle of width r and height h (the *stem*) [10, 9]. We define a Poincaré surface at the arc of the cap with negative momentum in the radial direction, i.e., just after the collision with the arc. For the coordinates of the Poincaré map, we use the angle θ (the origin is defined as the center of the cap) and the associated angular momentum L. This Poincaré map $\Phi(L, \theta)$ is area-preserving;

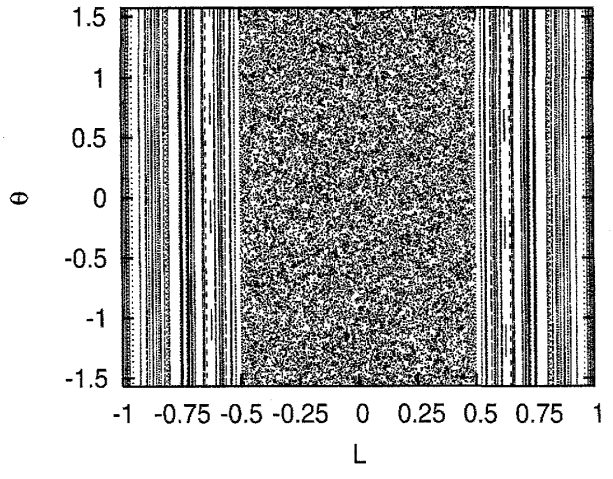

Figure 5: The Poincaré surface for $R = 1$, $r = 0.5$ and $h = 1$. The region $|L| < 0.5$ is chaotic and the other integrable.

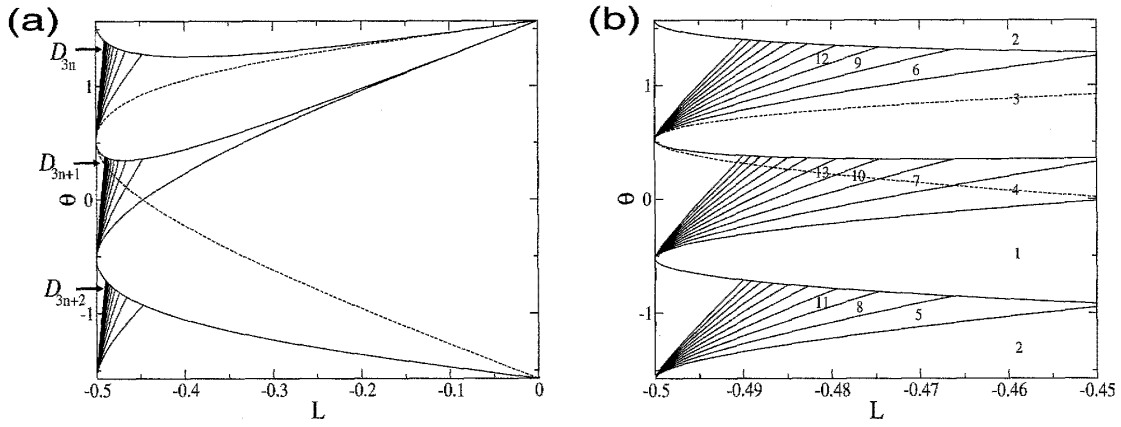

Figure 6: (a) The infinite partition constructed in terms of the escape time. The solid lines represent boundaries between regions with different escape times. The right side of the broken line is the injection domain where the trajectory which escapes from the cap returns again. The boundaries of the domains with the escape times longer than 32 are omitted. (b) A magnification of Fig. 6(a) in a neighborhood of the outermost tori ($L = -0.5$). Each number in the figure indicates the escape time of the domain where the number is located.

this fact can be proved through a direct calculation of the Jacobian of the map $\Phi(L, \theta)$, which turns out to be unity everywhere. This coordinate system is slightly different from the Birkhoff coordinates, because the Birkhoff coordinates are defined on the whole boundary of the billiard table, but here we take the Poincaré section only on the arc.

We display an example of the Poincaré surface in Fig. 5. The Poincaré map $\Phi(L, \theta)$ is defined on $\mathcal{D} = \{(L, \theta) \in [-R, R] \times [-\pi/2, \pi/2]\}$; the region $|L| < r$ is chaotic, and $|L| > r$ is filled with torus. The Poincaré map is symmetric with respect to the origin $(L, \theta) = (0, 0)$, i.e., $\Phi(L, \theta) = -\Phi(-L, -\theta)$. Thus, we will restrict the domain of the Poincaré map to the region of the negative angular momentum in order to simplify the discussion. Then we can construct an infinite partition on this Poincaré surface in terms of an escape time as shown in Fig. 6(a)(b) by solid lines. Here, the escape time is defined by the number of collisions with the wall until the particle escapes from the cap region. We would like to point out a similarity of Fig. 6(a) and (b) to Fig. 3(II) of the abstract model. In both cases, the infinite partitions in terms of the escape times exist. Moreover, the scaling properties (of the areas of the domains; see [25] for detail) in the mushroom billiard corresponds to the case $\beta = 2$ in the abstract model $\psi(x, y)$. For this parameter value ($\beta = 2$), the correlation function decays as $C(t) \sim 1/t$ (the power spectral density behaves as $S(f) \sim -\log(f)$.). The numerical simulation of the correlation function of the mushroom billiard is consistent with this rough prediction as shown in Fig. 7.

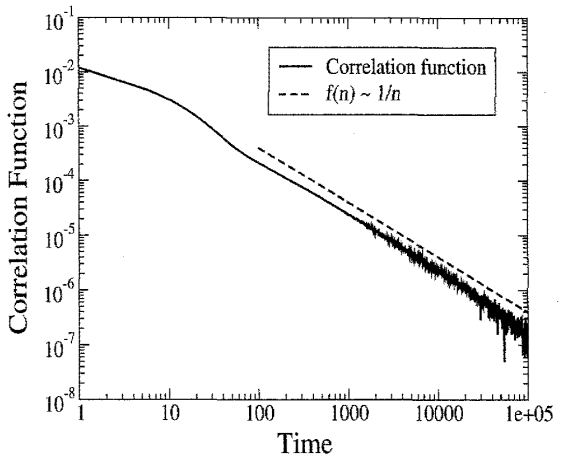

Figure 7: The auto-correlation function of the absolute value of the angular momentum $|L| - \langle |L| \rangle$ (the solid line) in log-log scale, where $\langle \cdot \rangle$ means the ensemble average in terms of the Lebesgue measure in the chaotic domain. The broken line represents a function $f(n) \sim 1/n$, which is a guide to the eye.

4 Summary

In this paper, we reviewed a piecewise linear map we have proposed in [24]. This model is a modified version of the map introduced by Tasaki and Gaspard [34, 35]. A main difference between our model and Tasaki-Gaspard model is the normalizability of invariant densities. The invariant density of the Tasaki-Gaspard model [34, 35] is not normalizable for a range of the parameter values. This is a typical property of dynamical systems with MUFPs [2, 1], and is caused by sticking motion in neighborhoods of the MUFPs. On the other hand, the uniform density is invariant for the map $\phi(x)$ presented in this paper; therefore the invariant density is normalizable for any values of the system parameters, even though our system has also a MUFP. This is because the present model has the mechanism suppressing injections of the orbits into neighborhoods of the MUFP and this property prevents divergences of the invariant density at the MUFP. As a consequence of the normalizability, the present model does not exhibit non-stationarity, which is generically observed in maps with MUFPs [1, 2, 34, 35]. The spectral properties of the FP operator of the present model is similar to those of the Tasaki-Gaspard model [34, 35]. There are two simple eigenvalues 1 and $\lambda_d \in (-1, 0)$; the former corresponds to the invariant eigenstate and the latter to the oscillating one. The eigenstate associated to λ_d, however, does not contribute to the long time behavior of the correlation functions because it decays exponentially fast. There is also a continuous spectrum on the real interval $[0, 1]$; this continuous spectrum leads to the power law decay of correlation functions.

Furthermore, the piecewise linear map $\phi(x)$ has been extended to an area-preserving invertible map $\psi(x, y)$ on the unit square. In contrast to the baker transformation, which is hyperbolic and shows exponential decays of correlation functions, this area-preserving map $\psi(x, y)$ is non-hyperbolic and displays a power law decay of correlations. As is well known, the mixed type Hamiltonian systems also exhibit a power law decay of correlation functions

[20, 11, 22, 23, 15, 38, 26]. Thus, the area-preserving map $\psi(x, y)$ might well be considered as an abstract model of the mixed type Hamiltonian systems in the following sense. Instabilities of the orbits of the map $\psi(x, y)$ [Eq.(6)] is weak in neighborhoods of the line $x = 0$, and the escape time from the left part $x < b$ to the right part $x > b$ diverges as $x \to 0$. In other words, the orbits stick to the line $x = 0$ for long times. This property seems to be similar to dynamics of Hamiltonian systems near torus, cantorus, and marginally unstable periodic orbits, where chaotic orbits become stagnant for long times. In fact, similar dynamics is observed in a Poincaré map of the mushroom billiard, which is a mixed type systems with sharply divided phase spaces [3, 4, 10, 9, 33], as reviewed in the second part of the present paper. This relation between the map $\psi(x, y)$ and a billiard system is similar to the relation between the baker map and the Lorentz gas [37].

Acknowledgement

Finally, I would like to note that our works reviewed here were strongly motivated by Prof. S. Tasaki's papers [34, 35, 36], in which he presented a rigorous mathematical analysis of nonlinear dynamical systems. Also, I would like to deeply thank him for helpful suggestions and encouragements.

References

[1] J. Aaronson. *An Introduction to Infinite Ergodic Theory.* American Mathematical Society, Province, 1997.

[2] Y. Aizawa, Y. Kikuchi, T. Harayama, K. Yamamoto, M. Ota, and K. Tanaka. Stagnant motions in hamiltonian systems. *Prog. Theor. Phys. Suppl.*, 98:36–82, 1989.

[3] E. G. Altmann, A. E. Motter, and H. Kantz. Stickiness in mushroom billiards. *Chaos*, 15:033105, 2005.

[4] E. G. Altmann, A. E. Motter, and H. Kantz. Stickiness in hamiltonian systems: From sharply divided to hierarchical phase space. *Phys. Rev. E*, 73:026207, 2006.

[5] V. I. Arnold and A. Avez. *Ergodic Problems of Classical Mechanics.* Benjamin, New York, 1982.

[6] R. Artuso. Anomalous diffusion in classical dynamical systems. *Phys. Rep.*, 290:37, 1997.

[7] R. Artuso and G. Cristadoro. Periodic orbit theory of strongly anomalous transport. *J. Phys. A*, 37:85, 2004.

[8] A. Ben-Mizrachi, I. Procaccia, N. Rosenberg, A. Schmidt, and H. G. Schuster. Real and apparent divergencies in low-frequency spectra of nonlinear dynamical systems. *Phys. Rev. A*, 31:1830, 1985.

[9] L. A. Bunimovich. Kinematics, equilibrium, and shape in hamiltonian systems: the lab effect. *Chaos*, 13:903, 2003.

[10] L. A. Bunimovich. Mushrooms and other billiards with divided phase space. *Chaos*, 11:802, 2001.

[11] B. V. Chirikov and D. L. Shepelyansky. Correlation properties of dynamical chaos in hamiltonian systems. *Physica D*, 13:395, 1984.

[12] J. R. Dorfman. *An Introduction to Chaos in Non-Equilibrium Statistical Mechanics.* Cambridge University Press, Cambridge, 1999.

[13] P. Gaspard. *Chaos, Scattering and Statistical Mechanics.* Cambridge University Press, Cambridge, 1998.

[14] T. Geisel, J. Nierwetberg, and A. Zacherl. Accelerated diffusion in josephson junctions and related chaotic systems. *Phys. Rev. Lett.*, 54:616, 1985.

[15] T. Geisel and S. Thomae. Anomalous diffusion in intermittent chaotic systems. *Phys. Rev. Lett.*, 52:1936–1939, 1984.

[16] I. M. Gel'fand and G. Shilov. *Generalized functions*, volume 3. Academic Press, New York, 1967.

[17] I. M. Gel'fand and N. Vilenkin. *Generalized functions*, volume 4. Academic Press, New York, 1964.

[18] H. H. Hasegawa and E. Luschei. Exact power spectrum for a system of intermittent chaos. *Phys. Lett. A*, 186:193, 1994.

[19] H. H. Hasegawa and W. C. Saphir. Unitary and irreversibility in chaotic systems. *Phys. Rev. A*, 46:7401, 1992.

[20] C. F. F. Karney. Long-time correlations in the stochastic regime. *Physica D*, 8:360, 1983.

[21] P. Manneville and Y. Pomeau. Intermittency and lorentz model. *Phys. Lett. A*, 75:1–2, 1979.

[22] J. D. Meiss and E. Ott. Markov-tree model of intrinsic transport in hamiltonian systems. *Phys. Rev. Lett.*, 55:2741, 1985.

[23] J. D. Meiss and E. Ott. Markov tree model of transport in area-preserving maps. *Physica D*, 20:387, 1986.

[24] T. Miyaguchi and Y. Aizawa. Spectral analysis and an area-preserving extension of a piecewise linear intermittent map. *Phys. Rev. E*, 75:066201, 2007.

[25] T. Miyaguchi. Escape time statistics for mushroom billiards. *Phys. Rev. E*, 75:066215, Jun 2007.

[26] T. Miyaguchi and Y. Aizawa. Anomalous diffusion in a hamiltonian system. *Prog. Theore. Phys.*, 109(1):145–149, 2003.

[27] M. Pollicott. On the rate of mixing of axiom a flows. *Invent. Math.*, 81:413, 1985.

[28] M. Pollicott. The differential zeta-function for axiom a attractors. *Ann. Math.*, 131:331, 1990.

[29] Y. Pomeau and P. Manneville. *Commun. Math. Phys.*, 74:189, 1980.

[30] D. Ruelle. Locating resonances for axiom a dynamical systems. *J. Stat. Phys*, 44:281, 1986.

[31] D. Ruelle. Resonances of chaotic dynamical systems. *Phys. Rev. Lett.*, 56:405, 1986.

[32] D. Ruelle. The thermodynamic formalism for expanding maps. *Commun. Math. Phys.*, 125:239, 1989.

[33] H. Tanaka and A. Shudo. Recurrence time distribution in mushroom billiards with parabolic hat. *Phys. Rev. E*, 74:036211, Sep 2006.

[34] S. Tasaki and P. Gaspard. Spectral properties of a piecewise linear intermittent map. *J. Stat. Phys.*, 123:803–820, 2002.

[35] S. Tasaki and P. Gaspard. Spectral properties of a piecewise linear intermittent map. *Physica D*, 183:205, 2003.

[36] S. Tasaki and P. Gaspard. Spectral characterization of anomalous diffusion of a periodic piecewise linear intermittent map. *Physica D*, 187(1-4):51 – 65, 2004.

[37] T. Tél and J. Vollmer. In D. Szász, editor, *Hard Ball Systems and the Lorentz Gas*. Springer-Verlag, Berlin ; Tokyo, 2000.

[38] G. M. Zaslavsky. Chaos, fractional kinetics, and anomalous transport. *Phys. Rep.*, 371:461, 2002.